Jurnal Teknik Sipil & Perencanaan 27 (2) (2025) p 39 - 48

JURNAL TEKNIK SIPIL & PERENCANAAN

10.15294/jtsp.v27i2/30023

http://journal.unnes.ac.id/nju/index.php/jtsp/index

Compressive Strength and Damage Simulation of Type V Cement-Based Concrete with GGBFS Addition

Audiyati Ishmata Hani'a[1, a)], Norma Puspita[2], and Marguan Fauzi[3]

[1]*Department of Civil Engineering, Faculty of Engineering, Diponegoro University, Semarang, Indonesia*
[2,3]*Civil Engineering Study Program, Faculty of Engineering, Indo Global Mandiri University, Palembang, Indonesia*

[a)] Corresponding author: audiyati.ishmata@live.undip.ac.id

Abstract. The durability of concrete structures in marine environments is often compromised by exposure to aggressive chemical agents. Although Type V cement is designed for high sulphate resistance, it remains susceptible to chloride penetration and magnesium-induced softening. This study investigates the mechanical performance of Type V cement-based concrete modified with GGBFS under simulated marine conditions. Specimens with 0%, 2%, 4%, and 6% GGBFS replacement were cast and cured in synthetic seawater for 7, 14, and 28 days before a compressive strength test. Experimental results showed that 2% GGBFS addition yielded the highest compressive strength of 48.12 MPa, which outperformed the regular concrete (42.32 MPa) at 28 days. Numerical simulations using the Mazars damage model in Cast3M were conducted to complement experimental findings, with mesh densities between 16 and 32 sides. Both experimental and modeling results were compared to BS EN 12390-3:2009 standards to categorize damage patterns. The analysis demonstrated that concrete with 2% dan 4% GGBFS exhibited satisfactory damage behaviour, while 0% and 6% GGBFS mixtures were classified as unsatisfactory. Further, the 16-sided mesh configuration generated damage patterns comparable to 2% and 4% GGBFS specimens, whereas the 32-sided mesh closely aligned with damage characteristics of 0% and 6% GGBFS concrete. This study highlights a novel experimental-numerical framework for optimizing GGBFS levels in marine conditions, demonstrating that integrated approaches effectively enhance performance evaluation and durability assessment.

Keywords: Concrete, Damage, Compressive Strength, GGBFS, Type V Cement, Marine Environment.

INTRODUCTION

The durability, safety, and sustainability of infrastructures, especially offshore concrete structures in marine environments, significantly suffer from the deterioration of cementitious and reinforced concrete [1]. Concrete exposure to maritime environments may lead to physical and chemical degradation. [2]. Chemical attacks, sulfate attacks, carbonation, alkali-aggregate reaction, and alkali-carbonate reactivity are the primary causes of these damages. Other external factors that play a significant role include abrasion, erosion, erosion cavitation, exposure to fire or prolonged high temperatures, and volume changes, all of which weaken the mechanical integrity and reduce the lifespan of a concrete structure. [3].

The stability and longevity of reinforced concrete structures are significantly compromised by sulfates in aggressive environments, as their effects lead to steel corrosion and concrete degradation [4]. Chlorides from de-icing salts are the leading cause of reinforcement corrosion, which produces expansive corrosion products around the reinforcing bars that expand volumetrically against the surrounding concrete. This expansion leads to cracking and spalling of the concrete cover, reducing the bond strength between concrete and steel [5]. As corrosion progresses, it reduces the rebar's cross-section and expands the steel volume, causing concrete damage and weakening the bond

between concrete and steel [6]. Additionally, sulfate attack on concrete involves reactions between external sulfate ions and cement minerals, causing expansion, cracking, strength loss, and eventual structural failure [7].

One of the most aggressive environmental factors that contributes to this deterioration is seawater, which contains a complex combination of chloride (Cl-), sulfate (SO42-), and magnesium (Mg2+) ions, in which these ions are capable of initiating both chemical and electrochemical reactions in concrete. [8]. The chemical effect of seawater on concrete is principally produced by the attack of Magnesium Sulfate (MgSO4), which is increased by the presence of Chloride content, hence inhibiting the expansion of concrete [9]. Although chloride ions can attack in a variety of ways, the majority of attacks are the result of an expansive chemical reaction (expansion) of a type of salt known as Friedls salt (Calcium Chloroaluminate), with the chemical formula for Friedls salt being (3CaO.Al2O3.CaCl2.10H2O) [10]. The quantity of this salt formed and expanded can vary from nominal to substantial, with concrete's higher water absorption capacity frequently facilitating this expanding reaction. In addition, Friedl's salt is produced by the seepage of Calcium Chloride solution into the concrete, with the CaCl that penetrates the concrete acting as the commencement of the material's softening [11].

Due to the corrosive properties of seawater and its potential to undermine concrete's chemical and mechanical integrity, it is essential to use binders with superior sulfate resistance. Within this context, Type V Portland cement has emerged as an appropriate option, specifically designed to resist sulfate attack by its low tricalcium aluminate (C_3A) content [5]. ASTM Type V cement concrete also demonstrates its superior long-term strength and durability with enhanced resistance to chloride penetration, corrosion, and freeze-thaw cycles, which is suited for rapid repair in an aggressive environment [12]. Prior research on the utilization of Type V cement was conducted by [13] To evaluate the sulphate resistance of self-compacting concrete, the results indicated that its compressive strength decreased due to its immersion in seawater for 28 days. Another tests were performed by [14] In the laboratory to study the possibility of limiting the mobility of soluble sulfate ions on the sulfate-contaminated crushed concrete base of a parking lot, as it began to experience severe heaving because of the secondary formation, expansive minerals (ettringite and thaumasite), in which the results showed that a blend of Type V cement and Class C fly ash offers a viable solution for stabilizing sulfate-contaminated crushed concrete. Furthermore, the properties of Portland cement mortar Type V, combined with Ground Rice Husk Ash (GRHA) and two types of limestone powder, were investigated. The results indicated that the compressive strength of the mortar decreased as the percentage replacement of GRHA and limestone in Portland cement Type V increased. According to the sulfate resistance results, it was found that the strength loss and drying shrinkage of the mortar were reduced as the percentage replacement of GRHA and LS in Portland cement Type V increased [15]. Extending Type V cement's resistance to sulfate-induced deterioration, it can be concluded that additional cementitious materials can be added to improve performance further.

GGBFS, or Ground Granulated Blast-Furnace Slag, has emerged as an eco-friendly cementitious material that improves the concrete's mechanical performance and durability when partially replacing portland cement and helps lower CO2 emissions linked to cement manufacturing [16]. GGBFS is a finely milled version of GBFS with cementitious characteristics similar to cement, allowing it to be used as an aggregate binder. GBFS is a hazardous material (B3 waste) derived from combustion residue in furnaces during the steel refining process or as a byproduct from steel plants, typically found in granular or sand-like form [17]. Its use in blended cement contributes to environmental benefits by reducing carbon dioxide emissions, preserving natural resources, improving waste management, and enhancing the properties and capabilities of concrete [18]. Therefore, GGBFS is one such supplementary material that has the potential to improve sustainability and performance while simultaneously reducing the environmental impact of Portland cement production [19]. A previous study investigated the use of GGBFS in the substitution of Portland Composite Cement (PCC), and the results indicate that the compressive strength of both the standard concrete and the GGBFS substitution concrete increases with age. In normal concrete, compressive strength values remain consistent; however, in concrete with GGBFS substitution, the compressive strength values start low but continue to rise, with an increase expected to continue after 28 days [20]. Another study explored the use of GGBFS as a partial replacement in cement concrete in cube, cylinder, and beam samples, with compressive strength tests performed utilizing compression test apparatus on 0%, 5%, 10%, and 15% fine aggregate replacement by GGBFS concrete; thus, the test results indicate that the compressive strength is significantly higher and almost identical when the fine aggregate content is substituted with GGBS at 5% and 15% [21]. The influence of Granulated Blast Furnace Slag on the compressive strength of mortar, manufacturing capacity, and economic value has been examined in a case study at PT. Semen Indonesia (Persero) Tbk., which discovered that using 2% granulated blast furnace slag resulted in the highest compressive strength at 28 days, whereas adding 0% provided the lowest compressive strength [22]. In addition, a study found that adding Ground Granulated Blast Furnace Slag (GGBFS) to Portland cement type II in an acidic environment increased the average compressive strength of the concrete. However,

treating with peat water in type II cement hinders concrete development due to sulfate attack, causing damage to the concrete [17].

Concrete damage refers to the physical and mechanical degradation caused by internal or external factors, reducing structural capacity and integrity. Microcracks, scaling, spalling, or changes in stiffness and strength can all be signs of this deterioration. It can be caused by mechanical loading (cyclic or impact forces), environmental exposure (such as chloride intrusion, sulfate attack, or freeze-thaw cycles), or chemical reactions (such as alkali-silica reaction or carbonation) [23]. Several strategies are used to analyze this decline, one of the most advanced being computational modeling by implementing damage mechanics models in Finite Element Analysis (FEA) software. Cast3M is a finite element-based tool that may be used to simulate concrete damage behaviour, with Mazars' damage, which can be used as the law to assist the simulation. [24], [25]. A previous study by [26] used the Mazars damage model in Cast3M to numerically evaluate oil palm shell concrete numerically numerically numerically, producing results compatible with experimental findings while showing the model's sensitivity to mesh density and geometric dimensions. It was also corroborated by [27] research describes that the failure patterns seen in cube specimen simulations revealed that adding finer mesh sizes within the random field framework provided results more closely approximating the experimental failure behaviour of oil palm shell concrete. In the other sample of concrete beams with single reinforced bar samples, cracking usually begins in the middle of the span. It remains unique throughout the loading period, with no new crack production but progressive spreading of the existing damage. [25]. Thus, the Mazars damage model's potential as a valuable instrument in structural damage simulations is further bolstered by the reliable and insightful representation of concrete failure patterns that the application of Cast3M provides.

Subsequently, it is reasonable to infer that the demand for high-performance binder systems that provide enhanced durability and sulphate resistance is increasing due to the aggressive chemical environment of marine environments, particularly the detrimental effects of seawater on concrete strength and integrity. Although Type V cement offers dependable protection against sulfate-induced deterioration, it is insufficient in its ability to withstand chloride ingress and magnesium-induced softening. Ground Granulated Blast Furnace Slag (GGBFS) and other supplementary cementitious materials have demonstrated promising potential in mitigating these limitations due to their pozzolanic and latent hydraulic properties. While numerous studies have explored the benefits of GGBFS in concrete, limited research has specifically addressed its integration with Type V cement under simulated marine conditions. Moreover, the application of numerical modeling, particularly using the damage model in Cast3M, to simulated damage behaviour in GGBFS modified with Type V concrete remains underexplored. Accordingly, this research aims to investigate the effect of GGBFS incorporation on the compressive strength and damage resistance of Type V cement-based concrete when exposed to seawater. To enhance the experimental investigation, numerical modelling will be conducted using Cast3M, employing the Mazars damage model across a range of mesh densities. The damage behaviour observed in the experimental and numerical studies will be benchmarked against [28] Standards to evaluate the performance and durability of the offshore and coastal environment.

MATERIAL AND METHODS

The study used a combined laboratory experiment and computational approach to assess the influence of Ground Granulated Blast Furnace Slag (GGBFS) on the compressive strength of Type V cement-based concrete under simulated marine conditions. To evaluate the structural response of concrete specimens under simulated environmental loading and analyze failure patterns, damage simulations were conducted using Cast3M in addition to physical testing. The primary objective was to investigate the impact of diverse GGBFS levels, specifically 0%, 2%, 4%, and 6%, on the strength and damage of concrete at various curing ages. Accordingly, the independent variable in this study was the percentage of GGBFS substituting for cement by weight, while the dependent variable was the resulting compressive strength. All variables are maintained constantly, including the water-cement ratio, aggregate gradation, blending method, curing regime, and specimen dimensions.

The materials used to fabricate concrete specimens complied with ASTM and SNI standards. According to [29], the binder consisted of Type V Portland cement from PT: Holcim Indonesia and GGBFS from PT. Krakatau Semen Indonesia. The coarse aggregate was pulverized aggregate from Merak with a nominal maximum size of 20 mm, while the fine aggregate was Pontianak river sand with a fineness modulus between 2.3 and 3.1. Both aggregates conformed to [30]. In addition, the seawater for curing was sourced from Lampung, and potable tap water from Sukamoro, South Sumatra, was employed as the blending water.

All construction materials were subjected to thorough quality control testing following SNI and ASTM standards before casting the specimens to ensure appropriateness and performance consistency. The fine and coarse aggregates

were initially tested for silt content using [31] and [32], as excessive fines can interfere with cement hydration and limit bonding effectiveness. Subsequently, the aggregate density and its interaction with the mixing water were evaluated through specific gravity and water absorption tests under [33] and [34]. These tests are essential for precise proportioning. The particle size distribution and the grading specifications were verified by conducting sieve analysis of both fine and coarse aggregates in accordance with [35].

A systematic mix design was developed to generate consistent compressive strength values across all GGBFS substitution levels, based on the results of preliminary material evaluations. Accordingly, cylindrical specimens with a diameter of 150 mm and 300 mm in height were cast using these materials, following the procedure outlined in [36]. All concrete mixes employed a fixed water-cement ratio of 0.45, in compliance with [37] for concrete exposed to fresh, brackish, and marine environments, and were prepared without chemical admixtures. The concrete composition was determined using. [29], and the detailed mix proportions are presented in Table 1 below.

TABLE 1. Concrete Mix Composition with GGBFS addition

Type of Concrete	Cement (kg)	Fine Aggregate (kg)	Coarse Aggregate (kg)	Water (kg)	Amount of GGBFS Addition (kg)
Normal Concrete	37.05	39.30	72.99	12.97	0.00
GGBFS Concrete 2%	37.05	39.30	72.99	12.97	0.74
GGBFS Concrete 4%	37.05	39.30	72.99	12.97	1.48
GGBFS Concrete 6%	37.05	39.30	72.99	12.97	2.22

Furthermore, after an initial 24-hour curing time at ambient temperatures, the concrete samples were demolded and immersed in synthetic saltwater that had been precisely manufactured in accordance with [38] to imitate the harsh chemical environment typical of marine exposure. To investigate the effect of exposure time on the material's mechanical performance, immersion durations were strategically established at 7, 14, and 28 days. Thirty-six cylindrical specimens were cast, representing a factorial combination of four GGBFS replacement levels (0%, 2%, 4%, and 6%) and three immersion durations. Three replicate specimens were assigned to each treatment group to ensure statistical consistency. A standardized evaluation of the structural performance and the assessment of GGBFS's contribution to concrete durability under simulated marine conditions was facilitated by subjecting all specimens to compressive strength testing following [39] upon reaching their designated curing ages. The total number of specimens cast for this study is summarized in Table 2.

TABLE 2. Distribution of concrete specimens based on GGBFS content and curing duration

Concrete Types	Curing duration (days)		
	7	14	28
Normal Concrete	3	3	3
GGBFS Concrete 2%	3	3	3
GGBFS Concrete 4%	3	3	3
GGBFS Concrete 6%	3	3	3

After completing the experimental program, the investigation was expanded to include computational simulations using Cast3M [24]. In which cylindrical concrete specimens measuring 150 mm in diameter and 300 mm in height, identical to those used in the physical tests, were subjected to simulated compressive loads. These simulations used different mesh densities to investigate stress distribution and failure behaviour under axial compression loads. The aggregate size utilized in the model ranges from 1 cm to 2 cm, per the recommendations outlined in [27]. These dimensional boundaries that reflect the minimum and maximum size serve as the basis for defining the structural pattern, as elaborated by [25]. Guided by these specifications, the simulation employed CUB8 solid elements, with mesh sizes calibrated directly to the aggregate dimensions. The aggregate size acted as a critical parameter influencing mesh granularity [27], thereby resulting in configurations comprising 32-sided and 16-sided mesh elements.

In addition, the Mazar damage model was employed to simulate the damage behaviour of the specimens; this model mathematically anticipates the structural response under the applied loading conditions until failure occurs due to strain localization. A single damage scalar variable, d, is defined by the model, with a range of 0 (undamaged) to 1 (fully damaged), as the material is regarded as isotropic. This damage value is computed through two underlying scalar variables: $\boldsymbol{d_t}$ and $\boldsymbol{d_c}$. To ensure the precise computation of these variables, it is necessary to identify the critical

material parameters that significantly affect the morphology and progression of tensile and compressive stress-strain curves [40]. These parameters include A_t and B_t for tensile response, and A_c and B_c for compressive response. The trial-and-error process is the source of all the parameters that were selected for the simulation, in which it also calibrates the chosen parameters, ensuring that the simulated global behavior closely matches the experimental observations [25], [41]. Subsequently, the simulation results will be compared against [28] to evaluate the conformity between experimentally observed damage behavior and the model prediction.

RESULT AND DISCUSSION

This section describes the compressive strength of concrete specimens subjected to simulated marine environments, with varying levels of GGBFS. The results are interpreted to assess the mix's performance over various curing periods, as detailed in the experimental design and testing procedures. The correlation between observed trends and the fundamental material behaviour is investigated to determine the impact of GGBFS substitution on strength development and its relevance to marine construction. The section also investigates the damage characteristics after the testing process, contrasting the results with [28] standards and Cast3M simulations at various mesh resolutions.

In the case of compressive strength, the results indicated that the various addition levels exhibited distinct performance trends. At 7 days, the 0% GGBFS blend demonstrated the highest early-age strength, while the 2% and 4% mixes demonstrated substantial gains by 28 days, indicating beneficial pozzolanic activity. These findings are reported in Figure 1, which shows each mix's average compressive strength values during all curing durations.

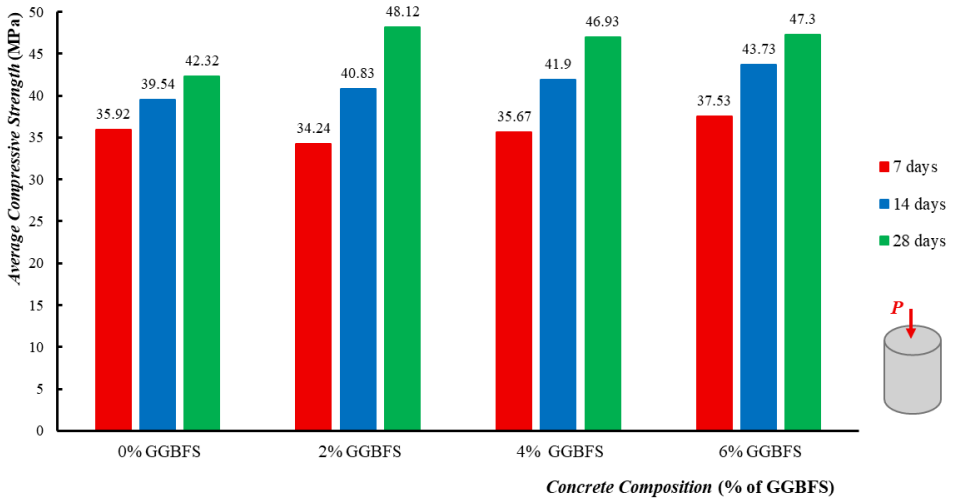

FIGURE 1. Compressive strength of concrete with varying GGBFS content at various curing ages

As illustrated in Figure 1, the compressive strength of concrete mixtures with 0%, 2%, 4%, and 6% GGBFS substitutions increased progressively over 7, 14, and 28 days of curing under simulated marine conditions. Notably, the 2% GGBFS mix substantially enhanced the strength of the concrete, reaching its peak at 48.12 MPa, outperforming both the standard concrete, which only reached 42.32 MPa, followed by the 6% and 4%, which were closely behind at 47.30 MPa and 46.93 MPa. Although its early-age strength was the lowest, the long-term gain suggests that 2% GGBFS incorporation offers an optimal balance between pozzolanic and matrix compatibility. At this dosage, sufficient calcium hydroxide remains available for secondary hydration. At the same time, the slag particles contribute to pore refinement and densification without disrupting the cementitious matrix, which is especially beneficial in chloride-rich environments. This optimal performance may also reflect a threshold effect, where minimal GGBFS addition enhances reactivity without causing dilution or retardation. Furthermore, the synergy between slag fineness and cement chemistry at 2% likely promotes efficient nucleation sites for C-S-H growth, accelerating strength development over time. These mechanisms are consistent with prior findings by [42], which indicates that excessive GGBFS content may reduce strength due to the dilution effect and increased availability of unreactive silica, which can trigger alkali-silica reactions and hinder matrix consolidation.

To further illustrate the strength development, the standard mix (0% GGBFS) showed a 10.10% rise between 7 and 14 days, followed by a 7.02% gain from 14 to 28 days, while the 2% GGBFS mix showed a more noticeable

strength trend, increasing by 19.26% from 7 to 14 days and 17.86% from 14 to 28 days. Compared to the standard concrete, this addition of 2% GGBFS in mixing exhibits a modest reduction in strength of −4.68% at 7 days. However, it significantly improved by 3.25% at 14 days and 13.71% at 28 days. Similarly, 4% of GGBFS concrete experienced a 17.48% increase from 7 to 14 days and a 12.00% increase from 14 to 28 days. Compared with the concrete without GGBFS addition, it demonstrated a minimal strength decline of -0.69% at 7 days, followed by subsequent increases of 5.97% and 10.89% at 14 and 28 days, respectively. Furthermore, the 6% of GGBFS mix increased strength by 16.54% between 7 and 14 days and 11.20% between 14 and 28 days, consistently exceeding the regular concrete at all ages with improvements of 4.48% at 7 days, 16.54% at 14 days, and 8.15% at 28 days. Thus, these results highlight the positive impact of low-percentage GGBFS substitutions, particularly those ranging from 2% to 4%, which show quicker strength growth and improved long-term performance under simulated maritime exposure.

Despite these strength gains, the concrete specimens also experienced substantial physical and chemical degradation due to prolonged exposure to the seawater environment. One of the most visible symptoms of degradation was the formation of surface cavities, which can be linked to the aggressive penetration of chloride ions and the leaching of calcium hydroxide from the cement matrix. This porosity not only compromises the structural integrity but also expedites the further ingress of detrimental ions. In addition, a distinct whitish layer was observed on the concrete surface, which is believed to be the result of lime (calcium hydroxide) deposits precipitated during the cement hydration process. These deposits may undergo additional reactions to produce calcite or other crystalline efflorescence when they come into contact with carbon dioxide and saline constituents. This phenomenon underscores the necessity of durable mix designs and suitable protective measures in coastal and offshore construction applications, particularly in unprotected or inadequately treated specimens, when it comes to concrete's susceptibility to marine exposure.

On the other hand, the failure patterns found at the end of the 28-day compressive strength tests were assessed in line with [28] to better understand the concrete specimens' damage behaviour. Per this standard, cylindrical specimens' fracture patterns are divided into two primary categories: satisfactory and unsatisfactory failures. The satisfactory category comprises four distinct varieties of fractures. At the same time, the unsatisfactory type incorporates eleven types designated as types A through K. Based on the experimental result and these standards, the concrete samples containing 2% and 4% GGBFS demonstrated satisfactory failure modes. In contrast, both the control samples (without GGBFS) and those with 6% GGBFS showed a relation to unsatisfactory failure characteristics. Figure 2 illustrates the visual evidence of these failure patterns.

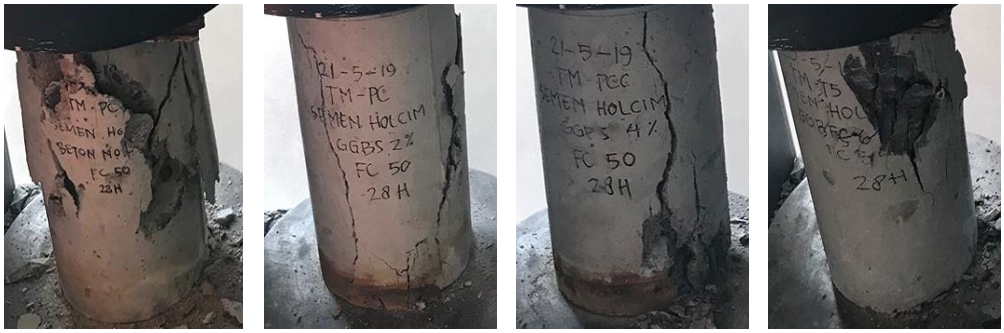

(a) (b) (c) (d)

FIGURE 2. The damage condition of 28-day concrete specimens at the end of the compressive test
(a) Normal concrete (without GGBFS) (b) Concrete with 2% GGBFS (c) Concrete with 4% GGBFS (d) Concrete with 6% GGBFS

Furthermore, the Cast3M simulations consistently replicated the damage observed after the 28-day compressive test, particularly in mesh configurations that employed 16 and 32-sided elements. The damaged zones were clearly colour-coded in the damage contour visualizations produced by the model, with orange signifying regions where concrete degradation had occurred and blue representing areas that remained structurally intact. This colour mapping was directly correlated with the binary damage state values, where 0 represented an undamaged state and 1 implied complete damage. The substantial visual distinction between damaged and undamaged areas aided intuitive interpretation and allowed for exact spatial analysis of damage concentration, distribution, and evolution within the specimen. This level of visual resolution improves the reliability of evaluating structural behaviour and integrity under simulated loading conditions, especially when distinguishing between satisfactory and unsatisfactory failure modes as indicated by standard categorization criteria in [28].

The simulation identified all samples with 0%, 2%, 4%, and 6% GGBFS as satisfactory failures, as assessed by simulations using the 16-sided mesh and compared to [28]. The cylindrical specimens, which were distinguished by damage concentrated at the mid-height, were divided into upper and lower portions as a consequence of this failure mode. These results indicate that the damage has been similar to that of concrete samples that contained 2% and 4% GGBFS, which exhibited this pattern upon satisfactory failure. The illustration of the damage pattern of the 16-sided mesh simulation can be seen in Figure 3.

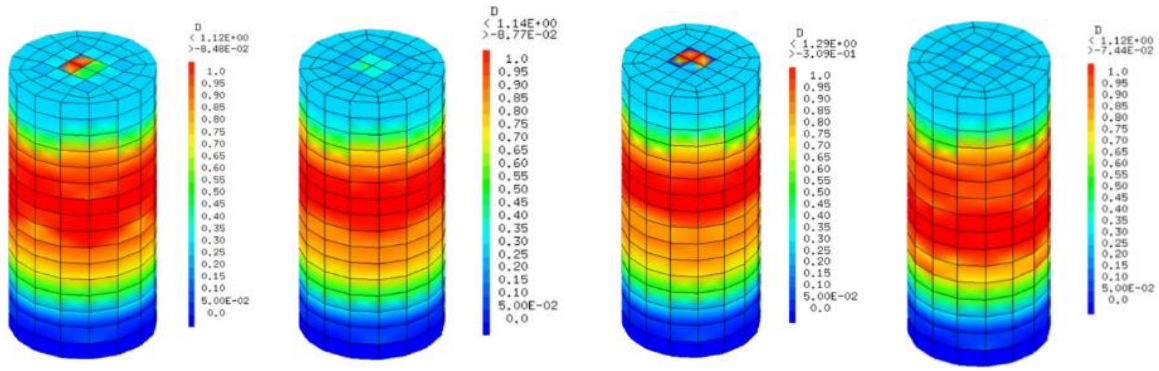

(a) (b) (c) (d)

FIGURE 3. Damage severity of 28-day concrete specimens after compressive test simulation:
(a) Normal concrete (0% of GGBFS) (b) Concrete containing 2% GGBFS (c) Concrete containing 4% GGBFS (d) Concrete containing 6% GGBFS

Nevertheless, the 32-sided mesh simulation uncovered damage patterns that were characterized as unfavourable across all mix compositions. Cracks were primarily concentrated from the top toward the concrete specimen's mid-height region, a Type J damage characteristic. According to the simulation, this pattern visually divided the specimens into two distinct components. Furthermore, this damage mode is aligned with the failure characteristics observed experimentally in plain concrete and specimens containing 6% GGBFS, both classified as unsatisfactory failures. The corresponding damage visualization from the 32-sided mesh simulation failure pattern is presented in Figure 4.

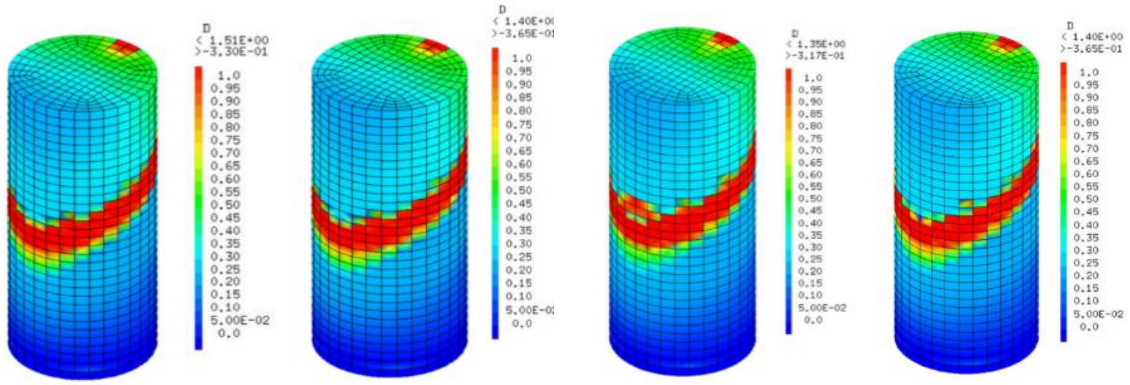

(a) (b) (c) (d)

FIGURE 4. Damage level of 28-day concrete specimens after compressive test simulation:
Control Mix (0% GGBFS) (b) GGBFS-modified mix (2%) (c) GGBFS-modified mix (4%) (d) GGBFS-modified mix (6%)

Although the Cast3M simulations demonstrated promising alignment with experimental results, minor discrepancies were observed in crack propagation and damage localization. These differences may be attributed to the model's assumption of material homogeneity, which overlooks the inherent heterogeneity of concrete, including aggregate distribution and interfacial transition zones. Additional sources of error may include mesh sensitivity, boundary condition simplifications, and the limitations of trial-and-error parameter calibration. Future studies should incorporate material heterogeneity into experimental design and numerical modeling to enhance simulation accuracy and better reflect real-world structural behaviour.

CONCLUSION

This study demonstrates the significant impact of GGBFS incorporation on the compressive strength and damage characteristics of Type V cement-based concrete under simulated marine exposure. The 2% GGBFS replacement achieved the highest compressive strength at 48.12 MPa after 28 days. Low to moderate GGBFS levels (2%, 4%, and 6%) consistently outperformed the control mix, enhancing early-age strength development and improving failure resistance in chloride-rich environments. The primary innovation of this study lies in integrating laboratory results with numerical simulations using the Mazars damage model in Cast3M. This approach remains rare in marine concrete research involving Type V cement. The simulation framework effectively replicated observed failure modes, with 16-sided mesh topologies accurately representing the satisfactory experimental mixtures (2% and 4% GGBFS), whereas 32-sided meshes more precisely captured the unsatisfactory characteristics of 0% and 6% mixes. Low GGBFS dosages between 2% and 4% are recommended for the practical application to improve early-age strength and degradation resistance. However, this study is limited by its short curing duration, which is only 28 days, focusing only on compressive strength. Future research should focus on examining the long-term durability, tensile behavior, and material heterogeneity to enhance the realism of simulations and facilitate the broader implementation of GGBFS-modified concrete in coastal infrastructure.

REFERENCES

[1] F. Qu, W. Li, W. Dong, V. W. Y. Tam, and T. Yu, "Durability deterioration of concrete under marine environment from material to structure: A critical review," *J. Build. Eng.*, vol. 35, no. December 2020, p. 102074, 2021, doi: 10.1016/j.jobe.2020.102074.

[2] F. P. Glasser, J. Marchand, and E. Samson, "Durability of concrete —Degradation phenomena involving," *Cem. Concr. Res.*, vol. 38, no. 2, pp. 226–246, 2008. https://doi.org/10.1016/j.cemconres.2007.09.015.

[3] [Y. P. Asmara, "Types and Causes of Concrete Damage," Springer Nature, 2023, pp. 25–44. https://doi.org/10.1007/978-981-99-5933-4_3.

[4] I. Xhaferaj and I. Dervishi, "Action of atmospheric agents against reinforced concrete," 2013, [Online]. Available: http://dspace.epoka.edu.al/handle/1/1282?show=full.

[5] I. Holly, K. Gajdosova, and R. Sonnenschein, "Reinforcement Corrosion and its Effect on Bond Behaviour," *Appl. Mech. Mater.*, vol. 837, no. June, pp. 179–182, 2016, doi: 10.4028/www.scientific.net/amm.837.179.

[6] A. S. Syll and T. Kanakubo, "Impact of Corrosion on the Bond Strength between Concrete and Rebar: A Systematic Review," *Materials (Basel).*, vol. 15, no. 19, 2022, doi: 10.3390/ma15197016.

[7] D. Zhang *et al.*, "Comparative analysis of sulfate resistance between seawater sea sand concrete and freshwater desalted sea sand concrete under different exposure environments," *Constr. Build. Mater.*, vol. 416, no. October 2023, p. 135146, 2024, doi: 10.1016/j.conbuildmat.2024.135146.

[8] D. Sun, Z. Cao, C. Huang, K. Wu, G. De Schutter, and L. Zhang, "Degradation of concrete in marine environment under coupled chloride and sulfate attack: A numerical and experimental study," *Case Stud. Constr. Mater.*, vol. 17, no. May, pp. 1–12, 2022, doi: 10.1016/j.cscm.2022.e01218.

[9] J. Wu, J. Wei, H. Huang, J. Hu, and Q. Yu, "Effect of multiple ions on the degradation in concrete subjected to sulfate attack," *Constr. Build. Mater.*, vol. 259, p. 119846, 2020, doi: 10.1016/j.conbuildmat.2020.119846.

[10] J. Ma, Z. Li, Y. Jiang, and X. Yang, "Synthesis, characterization and formation mechanism of friedel's salt (FS: 3CaO·Al2O3·CaCl2·10H2O) by the reaction of calcium chloride with sodium aluminate," *J. Wuhan Univ. Technol. Mater. Sci. Ed.*, vol. 30, no. 1, pp. 76–83, 2015, doi: 10.1007/s11595-015-1104-y.

[11] T. Li, H. Chen, T. Zhang, L. Liu, and Y. Zheng, "Thermodynamic study on phase composition of hardened Portland cement paste exposed to CaCl2 solution: Effects of temperature, CaCl2 concentration, and type and dosage of supplementary cementitious materials," *Cem. Concr. Res.*, vol. 178, no. January, p. 107437, 2024, doi: 10.1016/j.cemconres.2024.107437.

[12] N. Ghafoori, M. O. Maler, M. Najimi, and A. Hasnat, "Properties of high early-strength Type V cement concrete for rapid repair," vol. 289, p. 2003, 2019, doi: 10.1051/MATECCONF/201928902003.

[13] M. K. Putri, "The Effect of Portland Cement Type V due to Self Compacting Concrete (SSC) on Sulphate Resistance," Universitas Indonesia, 2011.

[14] S. L. Sarkar and D. N. Little, "Stabilization of Sulfate-Contaminated Crushed Concrete Base with Type V Cement and Fly Ash," *Transp. Res. Rec.*, vol. 1611, no. 1, pp. 3–9, 1998, doi: 10.3141/1611-01.

[15] B. Chatveera and P. Srinourn, "Properties of Portland Cement Type V Mortar Mixed with Ground Rice Husk

Ash and Limestone Powder," *IOP Conf. Ser. Mater. Sci. Eng.*, vol. 371, no. 1, 2018, doi: 10.1088/1757-899X/371/1/012008.
[16] G. E. Thomas, P. V. Indira, and A. S. Sajith, "Enhancement of Mechanical Properties of Cement Mortar Using Ground Granulated Blast Furnace Slag as a Partial Replacement," in *Lecture Notes in Civil Engineering (LNCE, Volume 274)*, Springer Nature, 2022, pp. 171–180. doi:10.1007/978-981-19-4055-2_15.
[17] N. Puspita, A. I. Hani'A, and M. Fauzi, "The effect of Ground Granulated Blast Furnace Slag (GGBFS) on Portland cement type II to compressive strength of high quality concrete," *IOP Conf. Ser. Mater. Sci. Eng.*, vol. 830, no. 2, 2020, doi: 10.1088/1757-899X/830/2/022068.
[18] R. A. T. Cahyani and Y. Rusdianto, "An Overview of Behaviour of Concrete with Granulated Blast Furnace Slag as Partial Cement Replacement," *IOP Conf. Ser. Earth Environ. Sci.*, vol. 933, no. 1, 2021, doi: 10.1088/1755-1315/933/1/012006.
[19] A. Moon *et al.*, "Experimental Investigation on Partial Replacement of Cement with Fly Ash and Glass Powder," *Int. J. Sci. Res. Eng. Manag.*, vol. 08, no. 05, 2024, doi: 10.1007/978-3-030-26365-2_7.
[20] [R. Raafidiani, S. Sumargo, and R. Permana, "The influence of Ground Granulated Blast Furnace Slag (GGBFS) as Portland Composite Cement (PCC) substitution in improving compressive strength of concrete," *IOP Conf. Ser. Mater. Sci. Eng.*, vol. 1098, no. 2, p. 022035, 2021, doi: 10.1088/1757-899x/1098/2/022035.
[21] P.Venkateswara Rao, Santhosh rajan. S.M, Hemalatha V, and Rakesh S, "Experimental Investigation on Partially Replacing the Fine Aggregate by using Ground Granulated Blast Furnace Slag in Cement Concrete," *Int. Res. J. Adv. Eng. Hub*, vol. 2, no. 04, pp. 870–874, 2024, doi: 10.47392/irjaeh.2024.0122.
[22] Samsuri, Ngudi, T, dan Chauliah, F. P., "Pengaruh Granulated Blast Furnace Slag dalam Semen Terhadap Kapasitas Produksi, Kuat Tekan Mortar dan Nilai Ekonomis: Studi Kasus di PT Semen Indonesia (Persero) Tbk," *Widya Tek.*, vol. 24, no. 2, pp. 67–71, 2016. https://doi.org/10.31328/JWT.V24I2.397.
[23] S. Murakami, *Continuum Damage Mechanics*, Volume 185., vol. 1, no. 69. Morikita Publishing Co. Ltd., Tokyo, 1967. https://doi.org/10.1007/978-94-007-2666-6.
[24] "Cast3M." http://www-cast3m.cea.fr/ (accessed Jun. 26, 2025).
[25] N. Handika and A. I. Hani'a, "Cracking Pattern Analysis of the Turning Band Method (Tbm) Application on a Single-Reinforcement Bar Concrete Beam Modelling Using the Mazars Damage," *J. Teknol.*, vol. 86, no. 6, pp. 95–105, 2024, doi: 10.11113/jurnalteknologi.v86.21817.
[26] K. Hongsen, M. Melhan, N. Handika, and B. O. B. Sentosa, "Parameterization of Oil Palm Shell Concrete on Numerical Damage Model Based on Laboratory Experiment using Digital Image Correlation," *J. Phys. Conf. Ser.*, vol. 1858, no. 1, 2021, doi: 10.1088/1742-6596/1858/1/012029.
[27] A. I. Hani'a, N. Handika, and S. Astutiningsih, "Impact of random field-Size effect using Turning Band Method (TBM) on damage behavior modelling of oil palm shell concrete under compression test," in *AIP Conference Proceedings*, Apr. 2024, vol. 3114, no. 1, doi: 10.1063/5.0203254.
[28] BS-EN-12390-3-2009, "British Standard BS-EN-12390-3-2009 Testing Hardened Concrete Part 3: Compressive Strength of Test Specimens," *BSI Group*. p. 20, 2009.
[29] ASTM C989 – 09, "Standard Specification for Slag Cement for Use in Concrete and Mortars," *ASTM Stand.*, vol. 44, no. 0, pp. 1–8, 2013, [Online]. Available: http://10.217.116.4/pdflink/astmpdf/ASTM103/ASTM/PDF/SEC4/VOL2/C989.PDF.
[30] ASTM C 33 – 03, *Standard Specification for Concrete Aggregates*, vol. 03. West Conshohocken: ASTM International, 2003.
[31] Badan Standardisasi Nasional, "SNI 03-4142-1996 Metode Pengujian Jumlah Bahan Dalam Agregat Yang Lolos Saringan No. 200 (0,075 Mm)," *Badan Stand. Nas. Indones.*, vol. 200, no. 200, pp. 1–6, 1996.
[32] ASTM C117 – 13, "Standard Test Method for Materials Finer than 75-um (No.200) Sieve in Mineral Aggregates by Washing." 2013.
[33] B. S. Nasional, "SNI 1969:2008 Cara Uji Berat Jenis dan Penyerapan Air Agregat Kasar," *Badan Standar Nas. Indones.*, p. 20, 2008.
[34] ASTM C127, "Standard Test Method for Specific Gravity and Water Absorption of Coarse Aggregate," *Am. Soc. Test. Mater.*, vol. 04, no. Reapproved, pp. 1–6, 2001.
[35] A. International, "C 136 - 06 Standard Test Method for Sieve Analysis of Fine and Coarse Aggregates," *ASTM Int.*, pp. 1–5, 2009, [Online]. Available: www.astm.org,.
[36] ASTM Internasional, "Astm C 192/C 192M-07," pp. 1–8, 2009, [Online]. Available: http://www.aci-int.org.
[37] SNI-03-2834, "Tata Cara Pembuatan Rencana Beton Normal," 2002.
[38] ASTM ASTM D1141-98, *"Standard Practice for the Preparation of Substitute Ocean Water," Annual Book of ASTM Standards, Philadelphia, 2004.* Philadelphia: ASTM, 2004.

[39] ASTM C39/C39M-01, “Standard Test Method for Compressive Strength of Cylindrical Concrete Specimens 1.”
[40] G. Pijaudier-cabot, J. Mazars, G. Pijaudier-cabot, J. Mazars, D. Models, and J. Lemaitre, “Damage Models for Concrete To cite this version : HAL Id : hal-01572309,” pp. 500–512, 2017.
[41] R. F. Hamon, “Model damage of MAZARS Code _ Aster Table des Matières,” 2013.
[42] J. Ahmad *et al.*, “A Comprehensive Review on the Ground Granulated Blast Furnace Slag (GGBS) in Concrete Production,” *Sustain.*, vol. 14, no. 14, 2022, doi: 10.3390/su14148783.